

The University of Bradford Institutional Repository

<http://bradscholars.brad.ac.uk>

This work is made available online in accordance with publisher policies. Please refer to the repository record for this item and our Policy Document available from the repository home page for further information.

To see the final version of this work please visit the publisher's website. Access to the published online version may require a subscription.

Link to publisher's version: <http://dx.doi.org/10.1111/j.2042-7158.2012.01539.x>

Citation: Paluch KJ, Tajber L, Corrigan OI et al (2012) Impact of process variables on the micromeritic and physicochemical properties of spray-dried porous microparticles, part I: introduction of a new morphology classification system. *Journal of Pharmacy and Pharmacology*. 64(11): 1570-1582.

Copyright statement: © 2012 Wiley

This is the peer reviewed version of the following article: Paluch KJ, Tajber L, Corrigan OI et al (2012) Impact of process variables on the micromeritic and physicochemical properties of spray-dried porous microparticles, part I: introduction of a new morphology classification system. *Journal of Pharmacy and Pharmacology*. 64(11): 1570-1582. , which has been published in final form at <http://dx.doi.org/10.1111/j.2042-7158.2012.01539.x>. This article may be used for non-commercial purposes in accordance with Wiley Terms and Conditions for Self-Archiving.

Impact of process variables on the micromeritic and physicochemical properties of spray dried porous microparticles Part I- Introduction of a new Morphology Classification System

*Krzysztof J. Paluch, Lidia Tajber, Owen I. Corrigan, Anne Marie Healy**

School of Pharmacy and Pharmaceutical Sciences

Trinity College Dublin, College Green, Dublin 2, Ireland.

To whom correspondence should be sent. Ph.: 00 353 1896 1444, Fax: 00353 1 896 2810
e-mail: healyam@tcd.ie

Abstract

This work investigates the impact of spray drying (SD) variables such as feed concentration, solvent composition and the drying mode, on the micromeritic properties of chlorothiazide sodium (CTZNa) and potassium (CTZK). Microparticles (MPs) were prepared using a Büchi B-290 and characterised using thermal analysis, helium pycnometry, laser diffraction, specific surface area (T_{BET}) analysis and scanning electron microscopy.

MPs produced under different process conditions presented several types of morphology. To systematise the description of morphology of MPs, a novel Morphology Classification System (MCS) was introduced. The shape of MPs was described as spherical-1 or irregular-2 and the surface was classified as smooth-A or crumpled-B. Three classes of morphologies of MPs were discerned visually: Class-I (nonporous) and classes II and III comprising differing types of porosity characteristics. The interior was categorised as solid-continuous- α , hollow- β , unknown- γ and hollow with microparticulate content- δ . NPMPs of CTZNa and CTZK, produced without recirculation of the drying gas, had the largest T_{BET} of 72.3 m²/g and 90.2 m²/g, respectively, and presented morphology of class 1BIII α . Alteration of spray drying process variables, particularly solvent composition and feed concentration can have a significant effect on the morphologies of the spray dried microparticulate products. Morphology may be usefully described using the MCS.

Keywords: spray drying, morphology, solvent, specific surface area, amorphous, nanoporous microparticles

1. Introduction

Particles characterised by a porous morphology have been reported to have advantageous properties over non-porous materials when formulated in a variety of dosage forms¹⁻³. Porous materials with a large surface area usually present favourable compaction properties⁴. Thus large surface area/porous materials may be considered to be useful as binders in tablet formulations. Materials with large specific surface areas and porosity may also be used as efficient carriers for liquids⁵. It was reported that rapidly dissolving tablets containing a solid dispersion of indomethacin and porous silica particles produced by co-spray drying presented favourable dissolution properties over tablets prepared from physical mixtures of indomethacin and porous silica⁶.

The production of excipient -free nanoporous microparticles (NPMPs) by spray drying from solutions was first reported for the hydrophobic active pharmaceutical ingredient (API), bendroflumethiazide⁷. Budesonide NPMPs for pulmonary delivery, were subsequently reported to have a large specific surface area ($10.5 \text{ m}^2/\text{g}$)⁸. The preparation of NPMPs of hydrophilic materials, for example carriers of raffinose and trehalose has also been described⁹, where the largest specific surface area, measured for both sugars, was approximately $44 \text{ m}^2/\text{g}$. The largest specific surface area of any NPMP system reported to date was for another hydrophilic material, sodium cromoglicate, and was $98 \text{ m}^2/\text{g}$ ³.

The above studies presented that the feed formulation and process conditions dictated the particle morphologies and these in turn were related to the functional properties of the NPMPs^{3, 8-10}. An attempt to classify the possible modes of particle formation during solvent evaporation was presented previously¹¹. This classification was based on the ability of a compound to crystallise and two major modes of particle formation were presented: one with distinct crystal habit and one without strong crystal habit. Another categorisation of morphologies of spray dried particles¹² distinguished three morphological types of particulates: agglomerate, skin-forming and crystalline. Inorganic materials were typically found to be crystalline and organics were mainly classed as skin-

forming. The study, unfortunately, did not include organic APIs. More recently a classification of morphological types of microparticles has been presented, which was not only to be applied to spray dried systems¹³. The microparticles were divided into those with a core, those with cellular structure, particles with embedded nanoparticles and composite shell as well as irregular with external voids and internal composition gradient. This classification, however, is difficult to apply when a thorough and systematic evaluation of porous particles is needed.

The goal of this work was therefore to systematise the description of the morphology of spray dried materials in general by introducing a novel morphology classification system (MCS) using four simple descriptors such as shape, surface properties, visual morphology and interior of the particle. Hydrophilic chlorothiazide sodium (CTZNa)¹⁴ and potassium (CTZK)¹⁵ were chosen as model compounds, on the basis of previous studies^{3, 9}, which indicated that porous microparticles of CTZNa and CTZK should be possible to obtain by spray drying from methanol/butyl acetate mixes. The studies entailed changing the feed concentration, methanol/butyl acetate solvent ratio and spray drying mode to methodically assess the impact of the various factors on morphology and other micromeritic properties including surface area of the NPMPs produced.

2. Materials and methods

2.1. Materials

Materials used in experiments were chlorothiazide (CTZ), potassium bromide (KBr, FT-IR grade) and PurpaldTM (Sigma Ireland), sodium hydroxide (NaOH, Riedel de Haën Germany), potassium hydroxide (KOH, Merck Germany). Solvents and other reagents: deionised water (Purite Prestige Analyst HP, Purite Limited, UK), acetone and ethanol (Corcoran Chemicals, Ireland), methanol and formic acid (Sigma, Ireland), n-propanol and ethyl acetate (Lab Scan, Ireland), butyl acetate (Merck, Germany), acetic acid, hydrogen peroxide, Hydranal-Composite and hydrochloric acid 32% (Riedel de Haën, Germany), nitric acid (BDH, UK), acetonitrile (Fischer Scientific, Ireland), sodium dihydrogen phosphate (Sigma-Aldrich, Ireland), phosphorus pentoxide desiccant (Fluka, Ireland).

2.2. Methods

2.2.1. Salts preparation

Chlorothiazide sodium (CTZNa DH) and potassium (CTZK DH) dihydrate and anhydrous CTZNa were obtained as previously described^{14, 15}. Anhydrous CTZK was obtained by spray drying of CTZK DH from water and secondary tray drying at 170 °C for 3 hours in an oven (Memmert UL 40, Germany).

2.2.2. Spray drying

Spray drying was performed using a Büchi B-290 Mini Spray Dryer (Büchi, Switzerland). An inert loop Büchi B-295 (for organic solvents) and additionally a dehumidifier Büchi B-296 (for water/organic solvent mixtures) were used for the closed mode operation. The spray dryer, depending on the sample, was used either in a closed mode with recirculation of nitrogen as the drying and nozzle gas or as an open system with nitrogen (open, suction mode) or in a mixed mode

where compressed nitrogen was used to atomise the solution but air was used as the drying gas (open, blowing mode). A standard atomization nozzle with a 1.5 mm cap and 0.7 mm tip was employed for each sample. The drying gas pressure of 6 bar at 4 cm gas flow (rotameter setting), equivalent to 473 norm litres per hour (nL/h) of gas flow in normal conditions ($p=1013.25$ mbar and $T=273.15$ K)¹⁶. The nozzle pressure drop was measured to be 0.41 bar. The pump speed was set to 30% (9-10 ml/min) and the aspirator was operated at 100%. Other conditions varied depending on the system spray dried and are summarised in Table 1.

The additional, secondary drying (AD) was performed in an incubator with forced air flow (Gallencamp economy incubator with fan, Weiss-Gallencamp, UK), using the same temperature as that of the outlet spray drying temperature for 12 hours for samples #19 and #20 (later referred to as #19* and #20*).

2.2.3. Physicochemical characterisation

Differential scanning calorimetry (DSC) and thermogravimetric (TGA) analyses were performed using a Mettler Toledo DSC 821^e and Mettler TG 50 module. Three measurements were carried out in vented aluminum pans, at a heating/cooling rate of 10 °C/min, under nitrogen purge¹⁴. True density was measured using helium (99.995% purity) AccuPyc 1330 Pycnometer MicromeriticsTM, presented results are an average of three measurements¹⁵. To image particles, a Mira Variable Pressure Field Emission Scanning Electron Microscope (SEM)¹⁵ was used. Measurements of particle size and particle size distributions were obtained using a laser diffraction particle sizer Mastersizer 2000 (Malvern Instruments, UK). Particles were dispersed using a Scirocco dry feeder instrument with 2 bar pressure. An obscuration rate of 0.5-6% was obtained under a vibration feed rate of 50%, results reported are the average of three analyses¹⁷. To determine the bulk specific surface area (T_{BET}) by Brunauer, Emmett, Teller (BET) isotherm a Micromeritics Gemini VI (USA) surface area analyzer was used. Each average result is calculated

on base of three measurements consisted of six steps, determining the amount of nitrogen adsorbed at 6 relative pressure points in the range of 0.05 to 0.3 of relative pressure P/P_0 with equilibration time of 10 s (free space was determined separately for each sample using helium gas, saturation pressure P_0 was determined prior to the measurement of each sample). Powder XRD (PXRD) analysis was conducted using a Miniflex II Desktop X-ray diffractometer. The tube output voltage used was 30 kV and tube output current was 15 mA. A Cu-tube with Ni-filter suppressing $K\beta$ radiation was used. Measurements were taken from 5 to 40 on the 2 theta scale at a step size of 0.05° per second in each case. Scans were performed at room temperature¹⁵.

2.2.4. Statistical analysis

Statistical analysis for the specific surface area (n=3), median particle size (n=3) and true density (n=3) data was carried out using the Minitab software. The Kruskal-Wallis test was carried out at a significance level of 0.05, with a p-value of less than 0.05 indicating that the observed difference between the means was statistically significant.

3. Results and discussion

3.1. Morphology and micromeritic properties of spray dried CTZNa and CTZK

All spray drying conditions employed for CTZNa and CTZK (Table 1) rendered PXRD amorphous materials, which was confirmed using DSC analysis¹⁹. Different morphologies of the spray dried particles were observed when spray drying conditions and solvent type were varied (Fig.1). Therefore, to facilitate the description of the different appearances, a morphology classification system (MCS) (Table 2) for spray dried compounds was developed. Firstly, the system introduces a code describing the shape of particles: 1 for predominantly spherical and 2 for irregular/non-spherical shape of particles. The second symbol indicates the surface description: A for smooth surface particle and B for crumpled particles. In the third place MCS describes the class of visual morphology with three different variants: I (nonporous), II (porous with nano-sized pores) and III (conglomerates of nanoparticles). The last symbol describes the interior of the particles and it is possible to distinguish: α for solid/continuous, β for hollow, γ for unknown and δ for hollow with nanoparticulate content. Examples of the various morphologies are presented in Table 3.

3.1.1 Spray drying from water

CTZNa (Fig. 1a) and CTZK (Fig. 1b) materials spray dried from water consisted of microparticles which were spherical in shape. CTZNa microparticles had smooth surfaces classified as 1AI α (Table 2, 3), while CTZK particles had a slightly crumpled morphology classified as 1BI α (Table 2). Imaging of spray dried samples #1 and #2, after grinding in an agate mortar revealed interiors of microparticles to be solid (Fig. 1 c, d). The difference in morphology may be attributed to difference in T_g between CTZK and CTZNa ~159 °C and ~192 °C respectively. In contact with residual water during final droplet solidification it is possible that CTZK develops higher degree of plasticity, reflected in the lower T_g of this material comparing to CTZNa. It has been reported that

materials with lower T_{gs} have a higher tendency to crumpling¹⁹ due to plasticisation effect²⁰. The crumpling in this case is not related to the saturation of the API in the solution feed¹³ since the aqueous solubilities of both salts are very similar^{14, 15}.

The true density of amorphous CTZNa microparticles (Table 4. #1) was $1.837 \pm 0.015 \text{ g/cm}^3$. The specific surface area by BET was $1.31 \pm 0.02 \text{ m}^2/\text{g}$ and the median particle size (d(50)) by laser diffraction was $2.6 \pm 0.1 \text{ }\mu\text{m}$. The true density of amorphous CTZK microparticles (Table 3. #2) was $1.872 \pm 0.003 \text{ g/cm}^3$, similar to that of CTZNa. The crumpled morphology of CTZK particles did not result in a change of specific surface area of the powder. It was measured to be $1.34 \pm 0.03 \text{ m}^2/\text{g}$, the same as for sample #1. The median particle size of CTZK of $3.1 \pm 0.1 \text{ }\mu\text{m}$ was slightly larger than that of CTZNa.

3.1.2. Spray drying from BA/MeOH systems

Different morphologies of the processed CTZNa were observed with a change in the MeOH/BA solvent ratio (Fig. 1. samples #3.-#9.). The change in morphology was reflected in the increased surface area of these powders (Table 4). Sample #10 spray dried from 100% methanol (a mix of particles of type 1AI β and 1BI β of MCS) had the smallest specific surface area (of those samples spray dried from non-aqueous solvents) of about $3.65 \pm 0.07 \text{ m}^2/\text{g}$ and it did not form porous particles (Fig. 1. 1 sample #10). The specific surface area of sample #10 was three times larger than that of sample #1 spray dried from pure water, most likely due to slight crumpling and lower particle size (Table 4).

The porosity of particles did not impact on the particle size. For example, sample #10 spray dried from 100% MeOH and CTZNa spray dried from a MeOH/BA 1:1 v/v mixture (#5, 1BII α of MCS) had similar median particle sizes of 1.6 and 1.7 μm , respectively. Overall, the median particle sizes for the CTZNa powders varied between 1.7 and 3.4 μm (Table 4).

The specific surface area by BET of the processed samples #1-10 showed that the largest surface area was determined for sample #6 (dried from a 3:2 v/v MeOH/BA mix) followed by sample #7 spray dried from a 7:3 v/v MeOH/BA solution with only a slightly, but significantly lower surface area (Table 4). Samples #6 and #7 presented morphology type of 1BII γ of the MCS. The smallest surface areas were measured for samples #9 and #10 spray dried from a 1:4 v/v MeOH/BA solvent mix and from pure methanol, respectively (Table 4). The particles of sample #9 were non-spherical, resembling shattered hollow and porous shells (Fig. 1k.) classified as 2AI α , while sample #10 was made of spherical but crumpled (1BI β) and smooth (1AI β) particles. A concentration of at least 20% v/v of BA was found to be critical for the formation of porous particles (Fig. 1j, #8, 2BII α). True density of the sample spray dried from methanol (#10) was significantly lower than the density of any CTZNa sample spray dried from mixed solvent systems (Table 4).

The feed solvent composition which resulted in the largest surface area for CTZNa was also used to spray dry CTZK. Anhydrous CTZK at 0.5% w/v concentration was spray dried in the same conditions as those used for sample #6 from a 3:2 v/v MeOH/BA solvent system (#11). Particles of #11 were spherical and porous with similar morphologies to sample #6 classified as 1BII γ of MCS (Fig. 1h). BET analysis of the spray dried material determined a specific surface area of $57.2 \pm 0.5 \text{ m}^2/\text{g}$. The median particle size was $2.0 \pm 0.1 \text{ }\mu\text{m}$ while the measured true density was $1.862 \pm 0.004 \text{ g/cm}^3$, slightly lower in comparison to sample #2 spray dried from water.

3.2. Effect of feed concentration and spray dryer configuration on particle morphology

The production of NPMPs from a solution containing 0.5% w/v of solids resulted in only 50 to 60% of the recovered dry material (with 1 g in the feed). An increase in the batch size to 10 g and higher required production yields greater than 60%. Low yield values would result in the loss of large amounts of processed material and clogging of the filter. One of the most important process

parameters, impacting directly on the production yield is the feed concentration¹⁹. Therefore the feed concentration was increased to the highest possible concentration not resulting in precipitation of the solid during feed preparation in ambient conditions. Experimentally this was established to be 2% w/v of anhydrous CTZNa or CTZK in MeOH. The content of BA was such that it did not result in precipitation of the API during processing (samples #12-#20). By increasing the feed concentration the production yield was increased to 75-80%. The change in feed concentration resulted in a decrease in T_{BET} of the spray dried CTZNa from $66.2 \pm 0.2 \text{ m}^2/\text{g}$ (sample #6) to approximately $42.6 \pm 0.4 \text{ m}^2/\text{g}$ (sample #15, 2BII α) when spray dried from 2% w/v solutions (Table 5). Readjustment of the optimal MeOH/BA ratio was thus required.

3.3. Postulated mechanism of NPMPs formation

It was postulated that, with an increased concentration of solute in the solvent/antisolvent mixture, in order to obtain the largest possible surface area, the proportion of the anti-solvent (BA) should be increased. The solid dissolved in the solvent/antisolvent mixture, due to solvent evaporation, starts to precipitate in the liquid environment (Fig. 2. 1a and 2 a). Preferential evaporation of MeOH (the solvent with the higher vapour pressure) results in spontaneous phase separation of nanoparticulates suspended in the solvent mixture (Fig. 2. 1b and 2b). The nanoparticles grow until separation of the solid from the solvent mix is complete (Fig. 2. 2c). Finally, due to evaporation of excess solvents, microconglomerates of nanoparticles are formed, described as morphology of type III (Fig. 2. 2d). Alternatively, if the volume of excess solvents is low, nanoparticles merge during growth (Fig. 2. 1c) prior to final separation of solid and final evaporation of solvents, forming morphology of type II (Fig. 2. 1d).

By changing only the proportion of the solvents, the greatest porosity and specific surface area was obtained for the material spray dried in the closed mode from 3:7 v/v MeOH/BA mixture - sample #12 (Table 5) classified as 1BIII α . For this sample, the change in

concentration of the solid in the feed from 0.5% to 2.0% altered remarkably the class of morphology from a mix of I and II (sample #3) to class III.

In general, increasing the ratio of MeOH:BA resulted in a reduction of porosity (as assessed from SEM). Material obtained using a MeOH/BA ratio of 7:3 (sample: #16) resulted in a morphology of type 2BII α , while a 4:1 v/v MeOH/BA ratio (sample #17) gave a morphology of class 1AI δ (Fig. 3). The sample spray dried from the MeOH/BA 3:2 v/v mix (#15, 2BII α) resulted in a larger surface area than that spray dried from MeOH/BA 1:1 v/v (#14, 1BIII α). An SEM image of #15 (2BII α) showed visually reduced porosity (class II of MCS) in comparison to sample #14 (Fig. 3- class III). Most likely the difference in T_{BET} was related to the non-spherical shape of the particles (class 2 of MCS) constituting systems #15 while #14 remained spherical belonging to class 1 of MCS.

The 3:7 v/v MeOH/BA solvent composition resulted in specific surface area values of $52.6 \pm 0.3 \text{ m}^2/\text{g}$ and $72.0 \pm 0.6 \text{ m}^2/\text{g}$ for CTZNa (sample #12- 1BIII α) and CTZK (sample #18- 1BIII α), respectively. Attempts to spray dry CTZK form I (monohydrate)¹⁵ from the 3:7 v/v MeOH/BA mixture resulted in only a 1% w/v feed concentration being achieved and a decreased surface area (of $33.5 \pm 0.3 \text{ m}^2/\text{g}$) when compared to sample #18.

Further process modification included changing the mode of the spray dryer from the closed to the open, blowing system to ascertain the feasibility of processing in a configuration similar to that used on an industrial scale²². This modification resulted in a further substantial improvement in the production yields to 90-95% (samples #19 and #20, both classified as 1BIII α). An additional increase in specific surface area of the materials to 72.3 ± 0.7 and $90.2 \pm 0.9 \text{ m}^2/\text{g}$ for CTZNa (sample #19) and CTZK (sample #20), respectively, was also seen (Table 5, Fig. 4. I).

Figure 4 II presents the relationship between $d(50)$ diameter of the particles and changing concentration of methanol in MeOH/BA mixtures for materials spray dried from two concentrations 0.5% w/v and 2.0% w/v. The diameters of the particles spray dried from the 2.0% w/v solutions are

about 1.4 times larger than of those spray dried from 0.5% w/v concentration (a 4-fold difference in concentration). This 1.4-fold difference is close to the theoretical ratio of 1.66 for a 4-fold increase in the initial feed concentration assuming that the particles are solid. It can be seen from figure 4 II that the d(50) diameter for sample #9 is significantly larger compared with diameters of other samples spray dried from the 0.5% w/v feed. For the samples (#12-#17) spray dried from the initial feed concentration of 2.0% w/v a difference in d(50) is statistically significant comparing with the equivalent samples spray dried from 0.5% w/v solutions (#3-#8). The Span values ranged from 1.2 to 1.9 and were, in general, smaller for the samples processed from 0.5% w/v solutions in comparison to the 2% w/v systems.

To calculate the diameter of a particle with the same T_{BET} as that measured for the powder, but assuming the non-porous nature of that particle, the concept of densest regular packing of spheres, assuming that the maximal degree of packing is 0.74²³ and the inverse relationship between the surface area and the radius²⁴ of the sphere were employed. The estimated particle diameters (ΦT_{BET}) are presented in tables 4 and 5. They corresponded well to the median particle sizes obtained from laser diffraction for nonporous samples (#1, 2 and 10) and gave a probable estimation of size of nanoparticulates constituting the NPMPs. The smallest ΦT_{BET} was estimated for sample #20, where the average diameter of nanoparticles forming the NPMPs was approximately 49 nm; this sample also had the greatest T_{BET} .

4. Conclusions

The novel Morphology Classification System of spray dried particles (MCS) developed was an efficient tool for morphology characterisation.

Spray drying is an effective method for producing amorphous MPs and NPMPs of chlorothiazide sodium and potassium salts (CTZNa and CTZK). Morphology of MPs was determined to be dependent on the type (water versus MeOH and MeOH/BA) and the ratio of solvents (MeOH/BA) used, the concentration of solid in the spray drying feed and the spray drying mode.

Samples spray dried from 0.5% w/v feed concentration comprised NPMPs mainly with morphology of class II. The use of 2% w/v feed concentration resulted in NPMPs with morphologies of class II and III. The particles spray dried from water had morphologies of type 1A1 α and 1B1 α for CTZK and CTZNa, respectively. The development of the different morphologies (A and B) for the aqueous samples was attributed to the different T_{gs} of the amorphous compounds (CTZNa: ~192 °C, CTZK: ~160 °C). NPMPs with specific surface areas of 72 m²/g and 90 m²/g for CTZNa and CTZK, 1BIII α of MCS respectively, were obtained with satisfactory yields (~90-95%) by spray drying from 2% w/v feed and a MeOH/BA (3:7 v/v) mixture. NPMPs with the largest specific surface areas presented morphology type III.

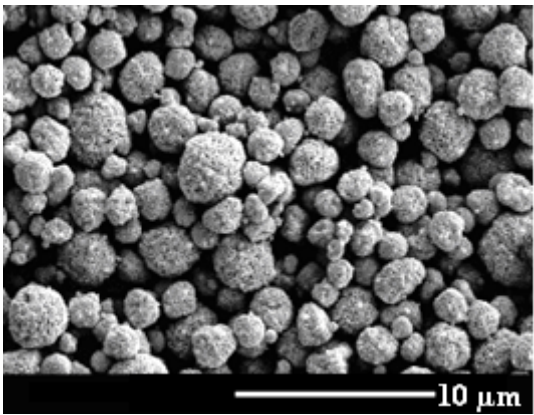
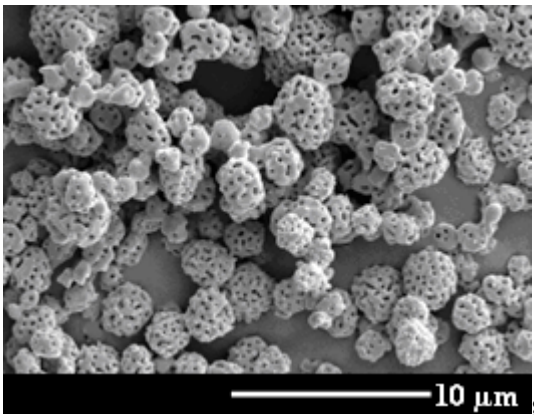
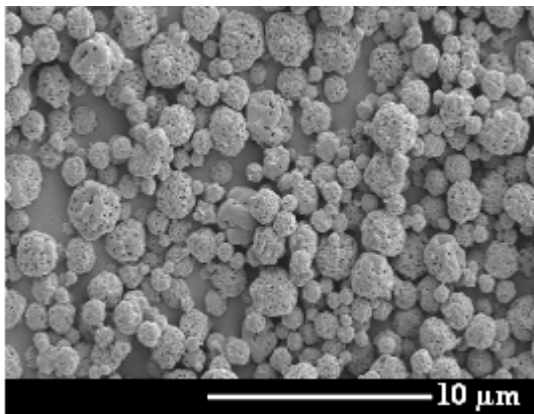
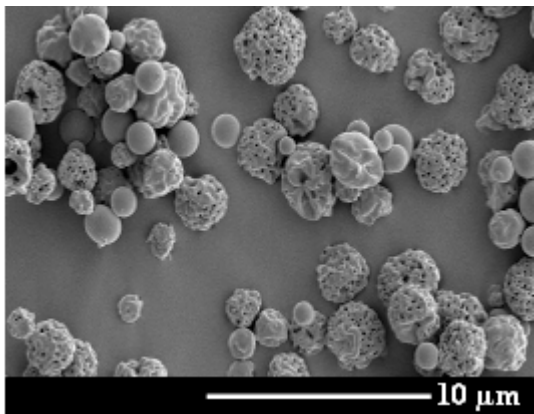
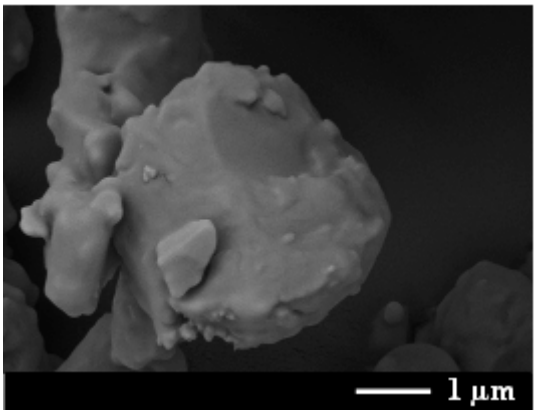
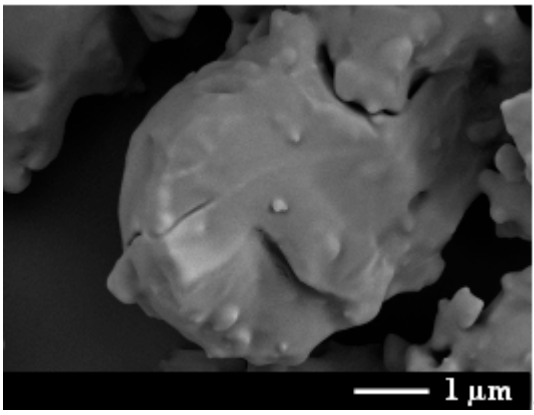
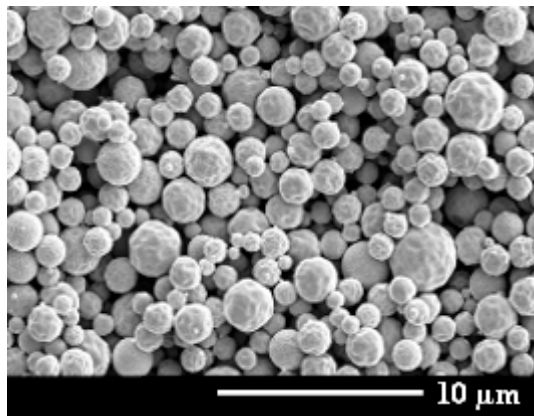
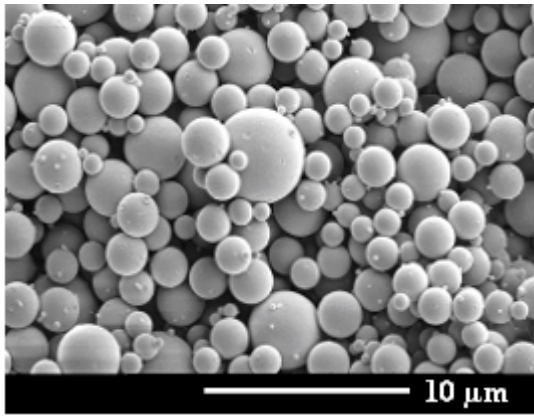
Acknowledgements

The authors wish to acknowledge funding for this research from the Irish Research Council for Science and Engineering Technology (IRCSET), the Solid State Pharmaceutical Cluster (SSPC), supported by Science Foundation Ireland under grant number [07/SRC/B1158] and the Irish Drug Delivery Research Network, a Strategic Research Cluster grant (07/SRC/B1154) under the National Development Plan co-funded by EU Structural Funds and Science Foundation Ireland.

References

1. Hirst PH et al. In vivo lung deposition of hollow porous particles from a pressurized metered dose inhaler. *Pharm Res* 2002; 19(3): 258-264.
2. Dellamary LA et al. Hollow porous particles in metered dose inhalers. *Pharm Res* 2002; 17(2): 168-174.
3. Nolan LM et al. Particle engineering of materials for oral inhalation by dry powder inhalers. II - sodium cromoglycate. *Int J Pharm* 2011; 405: 36–46.
4. Korhonen O et al. Effects of Physical Properties for Starch Acetate Powders on Tableting. *AAPS Pharm Sci Tech* 2002; 3(4): 1-9.
5. Carretero MI, Pozo M. Clay and non-clay minerals in the pharmaceutical industry Part I. Excipients and medical applications. *Appl Clay Sci* 2009; 46: 73–80.
6. Takeuchi H. Tableting of Solid Dispersion Particles Consisting of Indomethacin and Porous Silica Particles. *Chem Pharm B* 2005; 53(5): 487-491.
7. Healy AM et al. Characterisation of excipient-free nanoporous microparticles (NPMPs) of bendroflumethiazide. *Eur J Pharm Biopharm* 2008; 69(3): 1182-1186.
8. Nolan LM et al. Excipient-free nanoporous microparticles of budesonide for pulmonary delivery. *Eur J Pharm Sci* 2009; 37(5): 593-602.
9. Ní Ógáin O et al. Particle engineering of materials for oral inhalation by dry powder inhalers. I - Particles of sugar excipients (trehalose and raffinose) for protein delivery. *Int J Pharm* 2011; 405: 23–35.
10. Amaro MI et al. Optimisation of spray drying process conditions for sugar nanoporous microparticles (NPMPs) intended for inhalation. *Int J Pharm* 2011; doi:10.1016/j.ijpharm.2011.09.021

11. Leong HK. Morphological control of particles generated from the evaporation of solution droplets: Theoretical considerations. *J Aer Sci* 1987; 18(5): 511-24.
12. Walton DE, Mumford CJ. Spray dried products- characterization of particle morphology. *Trans I Chem* 1977; 77(Part A): 21–38.
13. Vehring R et al. Particle formation in spray drying. *Journal of Aerosol Science* 2007; 38: 728–746.
14. Paluch KJ et al. Physicochemical analysis of crystalline chlorothiazide and chlorothiazide sodium. *Eur J Pharm Sci* 2010; 41: 603–611.
15. Paluch KJ et al. Preparation and physicochemical analysis of crystalline forms of chlorothiazide potassium. *Eur J Pharm Sci* 2011; 42: 220–229.
16. Büchi 93001 en Operation manual Mini Spray Dryer B-290.
17. Tajber L et al. Spray drying of budesonide, formoterol fumarate and their composites-I. Physicochemical characterisation. *Int J Pharm* 2009; 367: 79–85.
18. Jones DS. Pharmaceutical statistics. 2002 London. Pharmaceutical Press.
19. Paluch KJ et al. Impact of process variables on the micromeritic and physicochemical properties of spray dried microparticles- Part II. Physicochemical characterisation of spray dried materials. *J. Pharm Pharmacol* 2012; *In Press*
20. Masters K. Spray drying in Practice 2002; *SprayDryConsult International* ApS., Denmark.
21. Hilfiker K. Polymorphism. 10.4.5. Influence of water content: Plasticization and chemical degradation. 2006 John Wiley & Sons.
22. Goula AM, Adamopoulos KG. Spray Drying of Tomato Pulp: Effect of Feed Concentration. *Dry Tech* 2004; 22(10): 2309-2330.
23. Steinhaus H. Mathematical Snapshots, 3rd ed. 1999 New York: Dover, pp. 202-203.
24. Gregg SJ, Sing KSW. Adsorption, Surface Area and Porosity. 2nd Edition, 1982 Academic press, London.



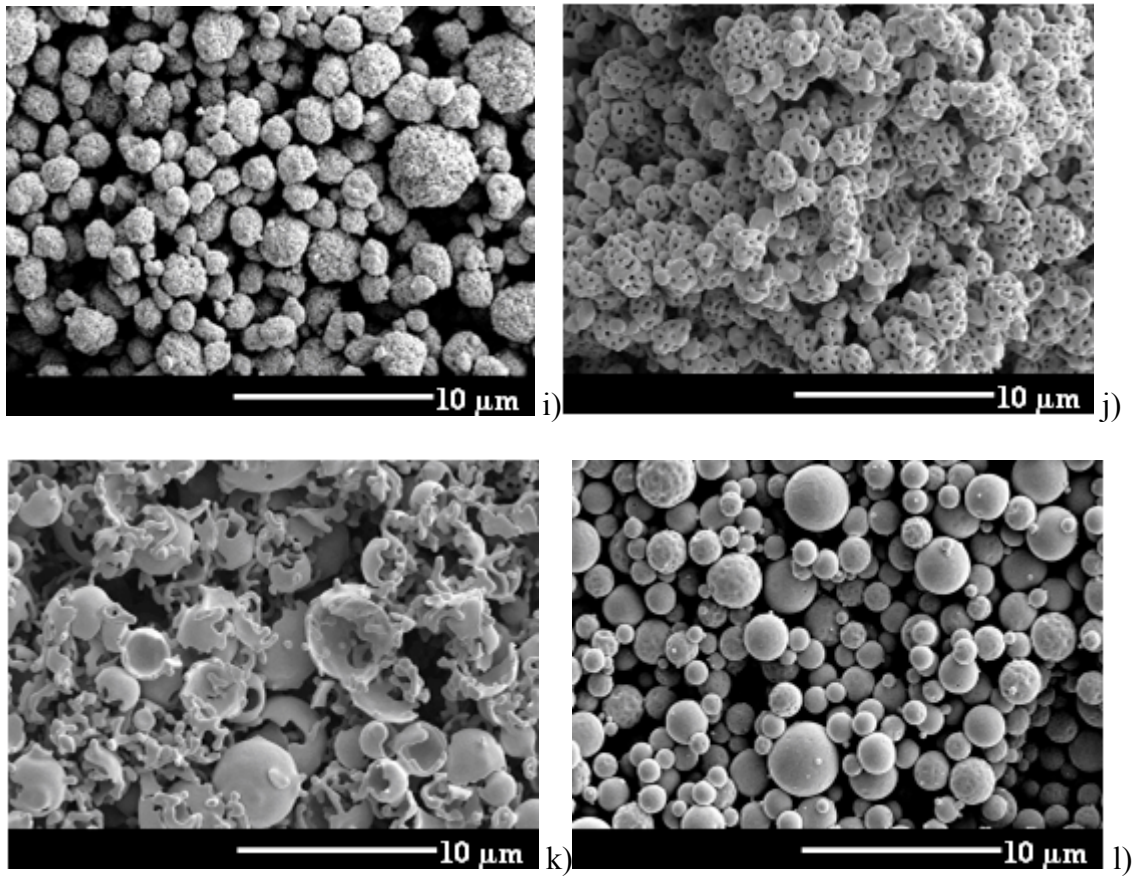


Fig. 1. SEM of CTZNa and CTZK spray dried samples: a) sample #1 (1AI α), b) sample #2 (1BI α), c) ground sample #1, d) ground sample #2 e) sample #3 (1BI α +1BII α), f) sample #4 (1BII α), g) sample #5 (1BII α), h) sample #6 (1BII γ), i) sample #7 (1BII γ), j) sample #8 (2BII α), k) sample #9 (2AI α) and l) sample #10 (1AI β +1BI β).

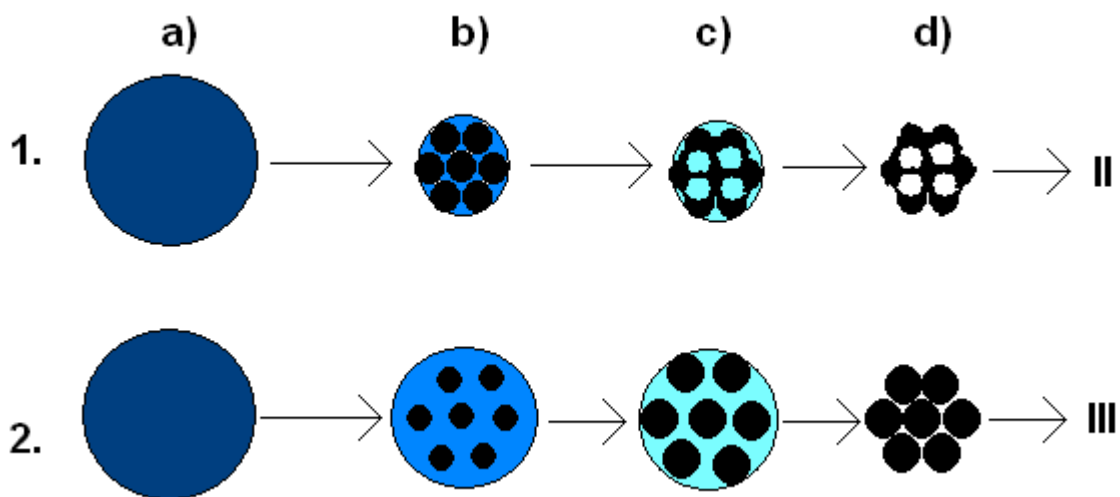


Fig. 2. Schematic formation of nanoporous microparticles. 1. Morphology of type II. 2. Morphology of type III. 1a, 2a- Droplet stage, 1b, 2b- Separation of solid phase (black), 1c- Bridging stage (bridging of nanoparticles due to further solid precipitation). 2c- Suspension stage (nanoparticles in a solvents mix), 1d- Evaporation stage- final evaporation of solvents. 2d- Microconglomeration stage- final evaporation of solvents and consolidation of nanoparticles. The brightening gradient of blue colour reflects a decrease in concentration of the solids in volume of solvents mix until final evaporation of excess of solvents mix- white voids remaining.

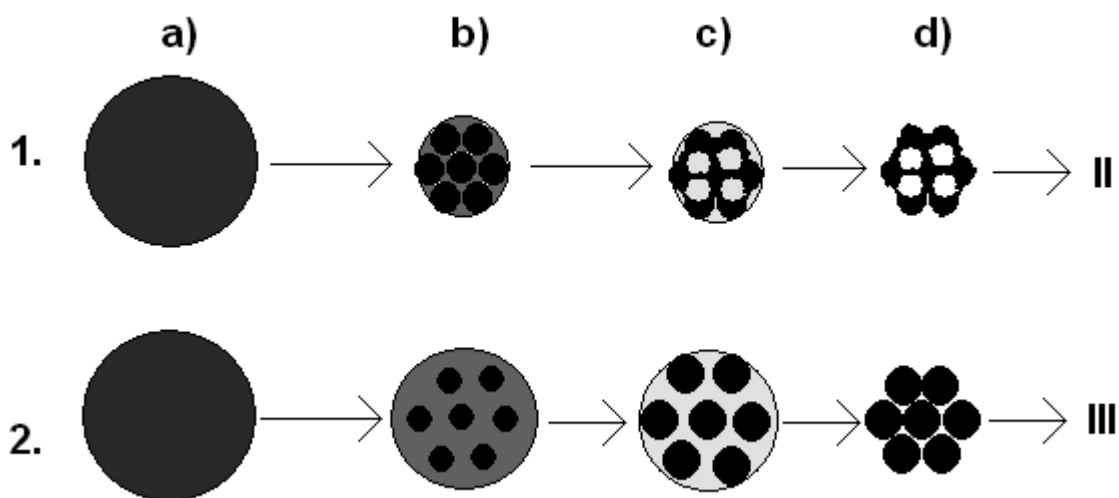


Fig. 2. Schematic formation of nanoporous microparticles. 1. Morphology of type II. 2. Morphology of type III. 1a, 2a- Droplet stage, 1b, 2b- Separation of solid phase (black), 1c- Bridging stage (bridging of nanoparticles due to further solid precipitation). 2c- Suspension stage (nanoparticles in a solvents mix), 1d- Evaporation stage- final evaporation of solvents. 2d- Microconglomeration stage- final evaporation of solvents and consolidation of nanoparticles. The brightening gradient of blue colour reflects a decrease in concentration of the solids in volume of solvents mix until final evaporation of excess of solvents mix- white voids remaining.

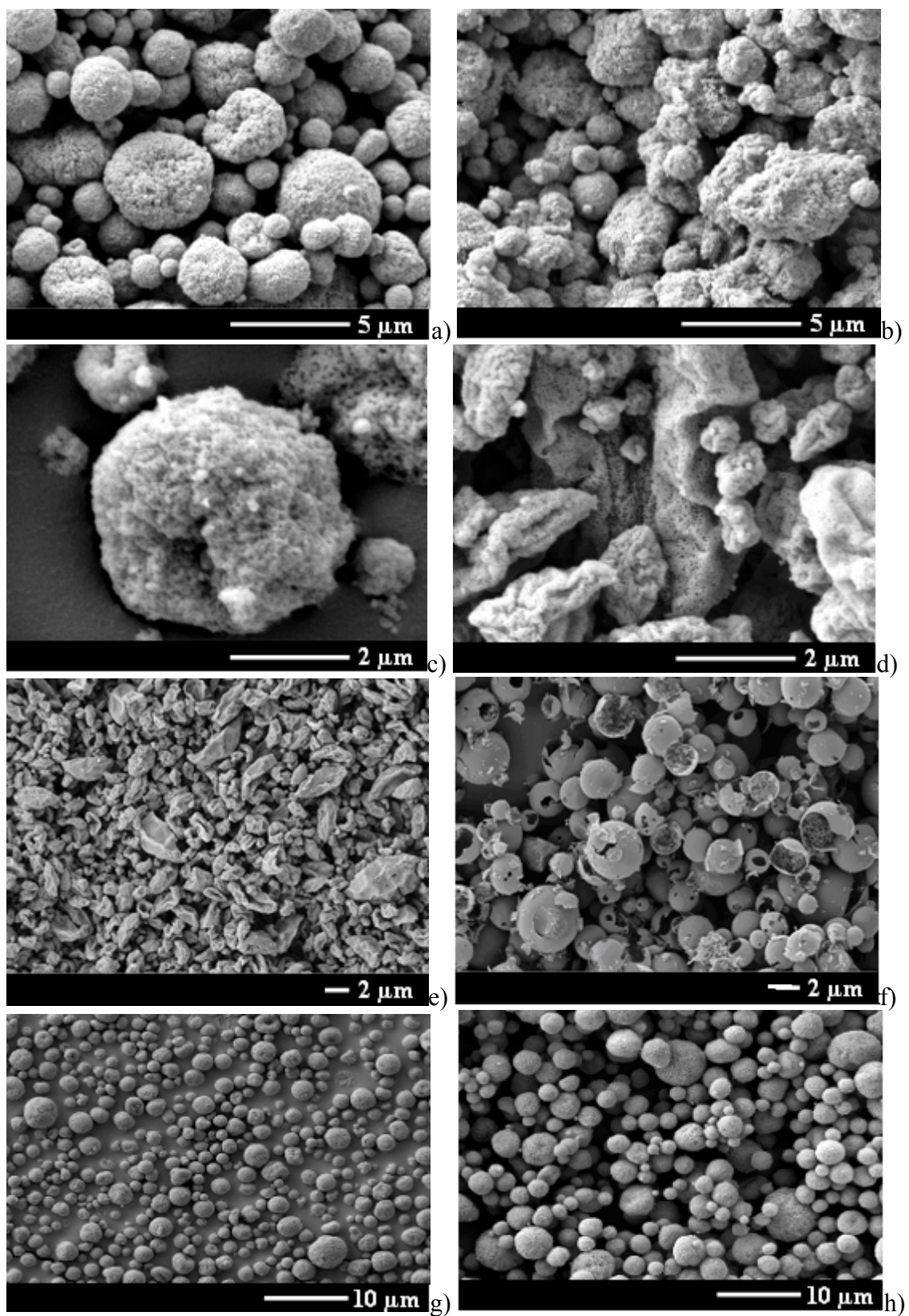


Fig. 3. SEM of CTZNa spray dried systems: a) sample #12 (1BIII α), b) sample #13 (2BIII α), c) sample #14 (1BIII α), d) sample #15 (2BII α), e) sample #16 (2BII α) and f) sample #17 (1AI δ), g) sample #19 and h) sample #20, both 1BIII α .

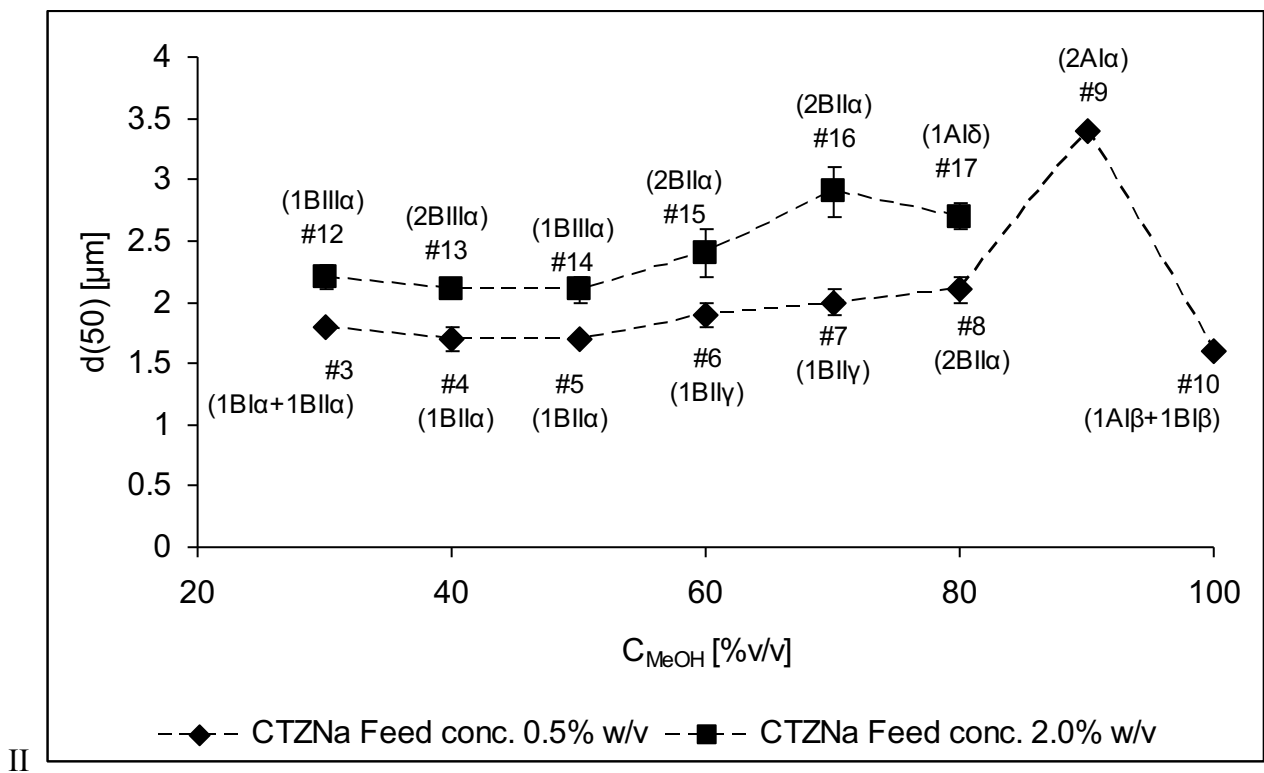
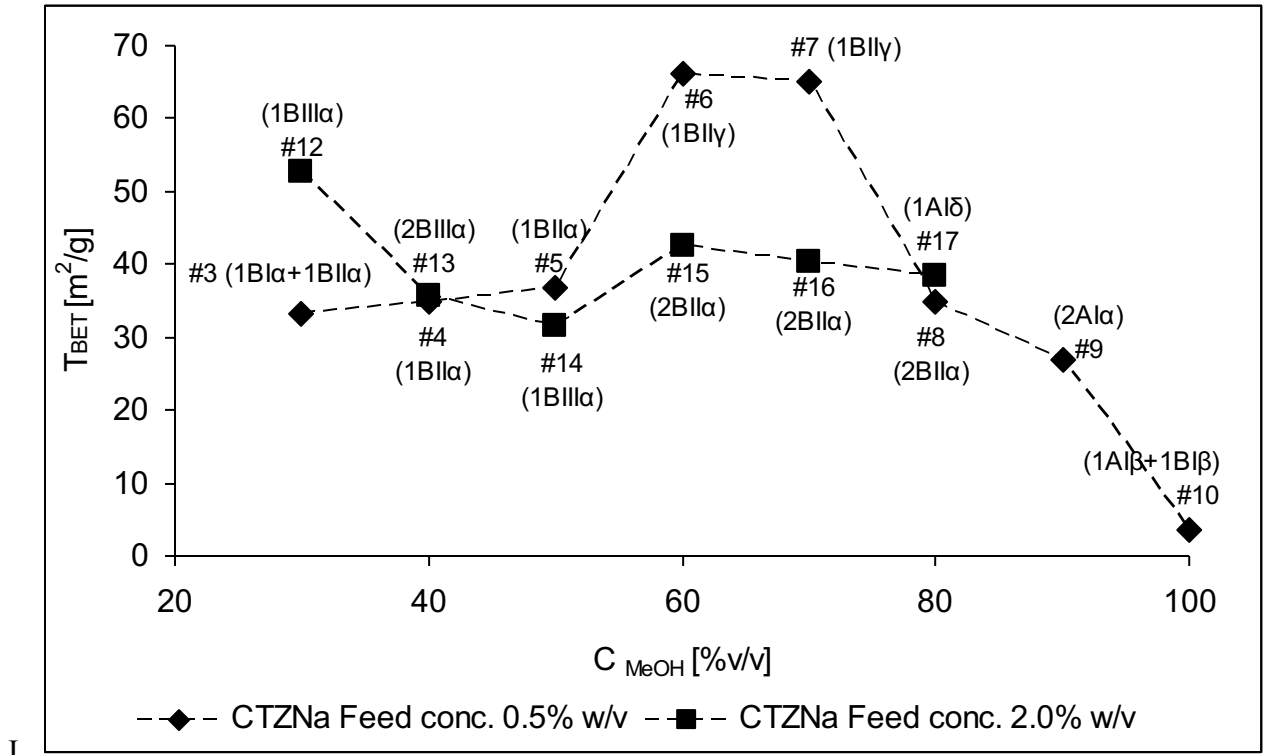


Fig. 4. I- Specific surface area T_{BET} and II- median particle size of CTZNa samples spray dried from different methanol concentrations.

Table 1. Spray drying conditions for CTZNa and CTZK samples. C_{MeOH} is the concentration of MeOH in the MeOH/BA solvent mixture.

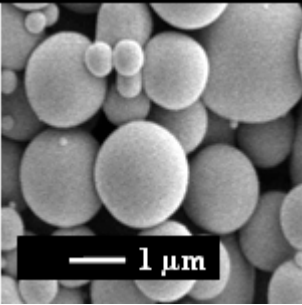
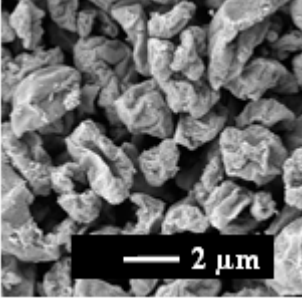
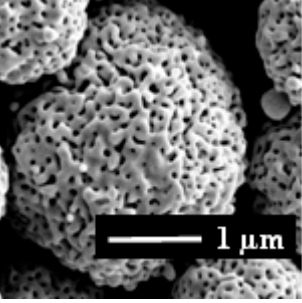
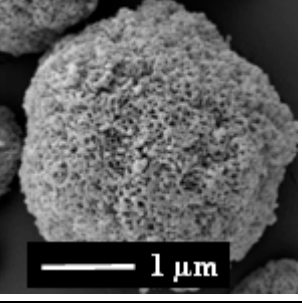
Sample (No #)	Solvent system	C_{MeOH} (%v/v)	Feed conc. (% w/v)	Inlet temp (°C)	Outlet temp (°C)	Mode*
#1. CTZNa	Water	-	2.0	160	99	OM-S
#2. CTZK	Water	-	2.0	160	101	OM-S
#3. CTZNa	MeOH/BA	30	0.5	120	87	CM
#4. CTZNa	MeOH/BA	40	0.5	120	92	CM
#5. CTZNa	MeOH/BA	50	0.5	120	97	CM
#6. CTZNa	MeOH/BA	60	0.5	120	98	CM
#7. CTZNa	MeOH/BA	70	0.5	120	98	CM
#8. CTZNa	MeOH/BA	80	0.5	120	98	CM
#9. CTZNa	MeOH/BA	90	0.5	120	99	CM
#10. CTZNa	MeOH	100	0.5	80,100	75,87	CM
#11. CTZK	MeOH/BA	60	0.5	120	97	CM
#12. CTZNa	MeOH/BA	30	2.0	120	98	CM
#13. CTZNa	MeOH/BA	40	2.0	120	98	CM
#14. CTZNa	MeOH/BA	50	2.0	120	98	CM
#15. CTZNa	MeOH/BA	60	2.0	120	99	CM
#16. CTZNa	MeOH/BA	70	2.0	120	100	CM
#17. CTZNa	MeOH/BA	80	2.0	120	101	CM
#18. CTZK	MeOH/BA	30	2.0	120	98	CM
#19. CTZNa	MeOH/BA	30	2.0	120	99	OM-B
#20. CTZK	MeOH/BA	30	2.0	120	99	OM-B

* OM-S – open, suction mode, OM-B – open, blowing mode, CM- closed mode.

Table 2. Elements of morphology classification system

Morphology classification system				
Example	1BIIα			
Classes of morphology	Shape	Surface	Visual morphology	Interior
	1. Spherical	A. Smooth	I. Nonporous	α . Solid/continuous.
	2. Irregular	B. Crumpled	II. Porous with nano-sized pores	β . Hollow.
			III. Conglomerates of nanoparticles	γ . Unknown
				δ . Hollow with nanoparticulate content

Table 3. Morphology Classification System (MCS) of spray dried particles.

Morphology type	Description of morphology	Morphology example
Shape		
1	Spherical	 (a)
2	Non-spherical, irregular	 (b)
Surface		
A	Smooth	(a)
B	Crumpled	(b)
Visual morphology		
I	Non-porous	(a)
II	Porous with nano-sized pores	 (c)
		 (d)

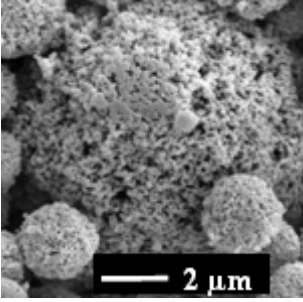
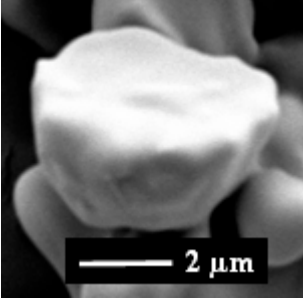
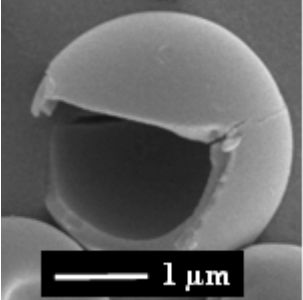
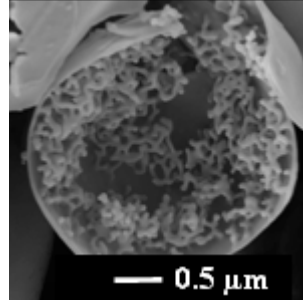
III	Porous, conglomerates of nanoparticles	
Interior		
α	Solid/Continuous	
β	Hollow	
γ	Unknown	(a)
δ	Hollow with microparticulate content	

Table 4. Specific surface area, particle size, true density results and particle diameter $\Phi(T_{BET})$ calculated from specific surface area of CTZNa and CTZK spray dried from methanol/butyl acetate mixtures.

Sample	Specific surface area [m ² /g]	Median particle size d(50) [μm]	Span	$\Phi(T_{BET})$ [μm]	True density [g/cm ³]
#1. CTZNa	1.31±0.02	2.6±0.1	1.8±0.1	3.418	1.837±0.015
#2. CTZK	1.34±0.03	3.1±0.1	1.8±0.2	3.418	1.872±0.003
#3. CTZNa	33.2±0.2	1.82±0.03	1.4±0.1	0.134	1.744±0.002
#4. CTZNa	34.8±0.2	1.7±0.1	1.4±0.1	0.128	1.734±0.004
#5. CTZNa	36.7±0.1	1.72±0.04	1.4±0.1	0.121	1.722±0.003
#6. CTZNa	66.2±0.2	1.9±0.1	1.41±0.03	0.067	1.727±0.004
#7. CTZNa	65.1±0.4	2.0±0.1	1.6±0.2	0.068	1.757±0.003
#8. CTZNa	34.8±0.3	2.1±0.1	1.43±0.02	0.128	1.747±0.002
#9. CTZNa	26.9±0.4	3.44±0.04	1.8±0.1	0.165	1.719±0.027
#10. CTZNa	3.7±0.1	1.62±0.03	1.22±0.06	1.201	1.473±0.001
#11. CTZK	57.2±0.5	2.0±0.1	1.42±0.02	0.078	1.862±0.004

Table 5. Micromeritic parameters of NPMPs spray dried from 2% w/v solid concentration and particle diameter $\Phi(T_{BET})$ calculated from specific surface area.

Sample	Specific surface area [m ² /g]	Median particle size d(50) [μm]	Span	$\Phi(T_{BET})$ [μm]
#12 CTZNa	52.6±0.5	2.2±0.1	1.81±0.06	0.084
#13 CTZNa	35.7±0.3	2.1±0.02	1.74±0.08	0.124
#14 CTZNa	31.5±0.3	2.1±0.1	1.91±0.06	0.141
#15 CTZNa	42.6±0.4	2.4±0.2	1.83±0.07	0.104
#16 CTZNa	40.4±0.4	2.9±0.2	1.8±0.1	0.110
#17 CTZNa	38.5±0.2	2.7±0.1	1.9±0.1	0.115
#18 CTZK	72.0±0.6	2.1±0.1	1.91±0.08	0.062
#19 CTZNa	72.3±0.7	2.9±0.03	1.9±0.1	0.061
#20 CTZK	90.2±0.9	3.1±0.1	1.9±0.1	0.049